Novel Architectures for High-Efficiency Amplifiers for Wireless Applications

Vesna Radisic, *Student Member, IEEE*, Yongxi Qian, *Member, IEEE*, and Tatsuo Itoh, *Life Fellow, IEEE*

***Abstract*— This paper presents three novel architectures for high-efficiency amplifiers relying on new harmonic-tuning techniques. These methods yield high-efficiency power amplifiers and reduce unwanted harmonic radiation from the transmitter front end. The first method uses the active integrated-antenna approach to perform harmonic tuning. The second method uses a nontraditional periodic microstrip filter, which allows broadband harmonic tuning. Finally, the third method combines the previous two approaches. Each technique is illustrated by a design example of a power amplifier integrated with an antenna. Guidelines for choosing the appropriate antenna structure and for designing the periodic structures are also presented. Another design issue is inclusion of the antenna and/or periodic structures into the amplifier simulation. To do this, a hybrid approach combining the finite-difference time-domain (FDTD) analysis and harmonic-balance simulation is employed.**

***Index Terms*— Active integrated antenna, cosite interference, PAE, power amplifier.**

I. Introduction

ADVANCED wireless communication systems require a compact and low-cost transmitter front end without sacrificing system performance. Crucial factors for wireless transmitters include efficiency, size, and bandwidth. Ways of achieving this are typically through high system integration and improved performance. However, this may cause increased electromagnetic interference (EMI) between transmitter subsystems. This paper presents new design techniques which specifically address these factors.

These goals are accomplished through increased integration between the amplifier and antenna. In a conventional system, the antenna is typically designed separately and connected to the amplifier by an interconnect, as shown in Fig. 1. Additionally, when multiple systems operating at neighboring frequencies exist in close physical proximity, there is an increasing EMI problem. To remedy this, a filter is often placed between the amplifier and antenna to reduce unwanted radiation. Traditionally, these components are designed with 50-Ω input and output impedance and connected together. This conventional method works well at low frequencies and when system design requirements are not tight. However, at high frequencies, interconnects become lossy and may possibly radiate or couple with other elements. This leads to the degradation of system performance even though individual components meet specifications.

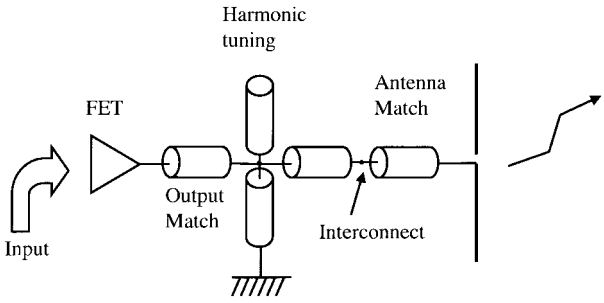

Fig. 1. Block diagram of a conventional transmitter front end. The amplifier and antenna are designed as separate subsystems matched to a 50-Ω environment.

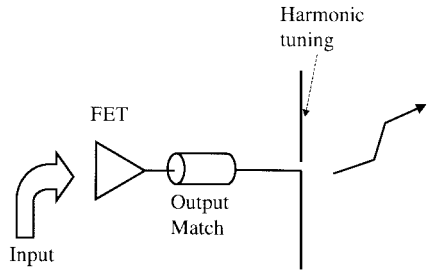

Fig. 2. Block diagram of an active integrated-antenna-transmitter front end.

One technique for reducing this problem is the active integrated-antenna approach [1]. In this method, the amplifier and antenna are combined into a single unit, as shown in Fig. 2. This concept can be used to explore new design topologies for the output stage. In this approach, the antenna can serve as filter, output matching circuit, and harmonic tuner in addition to being a load and radiating element. A key issue is that circuit components are not terminated in 50 Ω, but rather in the values that optimize system performance. The number of tuning or interconnecting elements between the amplifier and antenna can, therefore, be significantly reduced, with the effect of reducing system cost and losses.

High-power devices such as power field-effect transistors (FET's) or high electron-mobility transistors (HEMT's) typically have low output impedance, in some cases as low as 10 Ω, which is incompatible for 50-Ω systems. Therefore, device designers have been trying to increase the device output impedance toward 50 Ω at the expense of compromised output power. Similarly, antenna designers have been modifying antennas for 50-Ω match as well. This dilemma can

Manuscript received April 13, 1998; revised July 24, 1998. This work was supported by the U.S. Army, MURI Low-Power Low-Noise Electronics for Mobile Wireless Communication under Contract DAAH04-96-1-0005.

The authors are with the Electrical Engineering Department, University of California at Los Angeles, Los Angeles, CA 90095 USA.

Publisher Item Identifier S 0018-9480(98)08335-5.

be circumvented if the amplifier and antenna are combined together. Many planar antennas such as the microstrip patch or slot antenna can be designed for low input impedance and good radiation characteristics when operated near resonance. Therefore, the antenna and amplifier can be combined together with minimal matching circuitry in between.

Perhaps the most crucial factor in power-amplifier design is increasing efficiency. Typically, most of the system power is consumed in the output power-amplifier stage. Since higher dc power adds to both system cost and weight, power-added efficiency (PAE) of the amplifier has to be maximized. Traditionally, this is done by using harmonic tuning, which reflects harmonic power back to the device [2]. Recently, biasing schemes have been reported for increasing PAE [3]. This technique optimized the power-supply voltage in accordance with the input signal level to reach maximum PAE.

There are several techniques in harmonic tuning. Typically, higher order harmonics contain only a small amount of power. For this reason, practical designs usually terminate only second and third harmonics. Traditionally, tuning of the second harmonic is done by adding a quarter-wavelength (at the fundamental frequency) short-circuited stub at the output [4], [5]. Typically, this is most often placed at the drain bias line. At lower frequencies, this stub may use considerable circuit space. However, chip capacitors can also be used for rejection of the second harmonic if they have a self-resonance at the second harmonic [6]. Similar methods are used for tuning of the third harmonic. In this paper, we present several alternative methods for harmonic tuning. If designed properly, these methods offer a compact design.

The first of these approaches is the active antenna approach. If the antenna input impedance is purely reactive (or zero) at harmonic frequencies, it can be used to tune harmonics. This has been demonstrated in [7]. In this case, tuning of the second harmonic with an integrated antenna was shown to increase the PAE by 7%. There are additional benefits to this approach. In addition to increased PAE or output power of the amplifier, a reduction of unwanted harmonic radiation that causes EMI and ultimately degrades system performance can be observed.

The previously mentioned harmonic-tuning techniques are typically narrow-band. Some high-performance communication systems, for example those using multicarrier broad-band code-division multiple-access communication (CDMA), require high-efficiency broad-band power amplifiers. Broad-band harmonic tuning can be achieved using a microstrip filter based on the photonic bandgap (PBG) concept [8]. PBG is a periodic structure which prohibits wave propagation in certain frequency bands. Original PBG research was done in the optical region [9], but PBG properties are scalable and applicable to a wide range of frequencies. In the microwave region, PBG structures have been used in design of antennas [10], cavities [11], frequency-selective surfaces, and many other structures. In this paper, two-dimensional (2-D) structure based on etching a periodic 2-D pattern in the microstrip ground plane is used [12]. This structure has a stopband that is generally wider than can be achieved by using a single or double stub. This periodic structure is added between the antenna and amplifier. This configuration has an additional component, but can be used for broad-band operation.

The analysis of active antenna amplifiers is quite challenging. Traditionally, nonlinear analysis such as harmonic balance is used to analyze power amplifiers. This kind of simulation cannot analyze antennas or PBG structures, in which a three-dimensional (3-D) full-wave solution of Maxwell's equations is usually required. In this paper, the finite-difference time-domain (FDTD) technique is used because it can simulate arbitrary 3-D structures and provide broad-band frequency response with one simulation. FDTD results can then be incorporated into nonlinear circuit design to analyze the whole structure.

The amplifier design examples consist of class-AB, class-B, and class-F amplifiers, which are prevalent at microwave frequencies. However, with increasing device technology, other potentially higher efficiency types of amplifiers have been reported at microwave frequencies. Recently, a class-E amplifier has been realized at 1 GHz with 73% PAE and output power of 0.94 W [13]. In this case, approximate class-E operation is achieved by open circuiting the second harmonic only. More recently, a four-element integrated-antenna array with class-E performance was demonstrated at 5 GHz [14]. Output power greater than 33 dBm was demonstrated with a PAE of 65%. These classes of amplifiers are also expected to benefit from the above techniques.

II. Harmonic-Tuning Techniques

A. Active Integrated-Antenna Approach

Choice of antenna is of crucial importance in the active integrated-antenna approach. For minimization of interconnects, planar-type antennas such as the patch or slot are a good choice because they are suitable for direct integration with microstrip or coplanar waveguide (CPW). Typically, when considering an antenna, the antenna designer is interested in the antenna characteristics only at the system operating frequency. However, when the antenna is used for harmonic tuning, antenna characteristics over a broad frequency span must be considered. These characteristics fall into two categories. The first characteristic, input impedance at operating frequency and higher harmonics, must be chosen to maximize amplifier performance. The second characteristic, radiation properties of the antenna, is chosen for optimal wireless performance.

Input impedance of the antenna is a crucial part of the antenna design. First, this means that the input impedance at the fundamental frequency should be close to the optimum output impedance of the amplifier for maximum PAE or P_{out}. Additionally, the antenna should present a reactive termination at undesired higher harmonics. This second constraint is contrary to many planar antennas. For example, resonant higher modes of the rectangular patch antenna roughly occur at multiples of the fundamental resonance. Unless modified, this antenna is not particularly suited for harmonic tuning.

For optimal wireless performance, radiation properties of the antenna are also crucial. The antenna should have reasonable

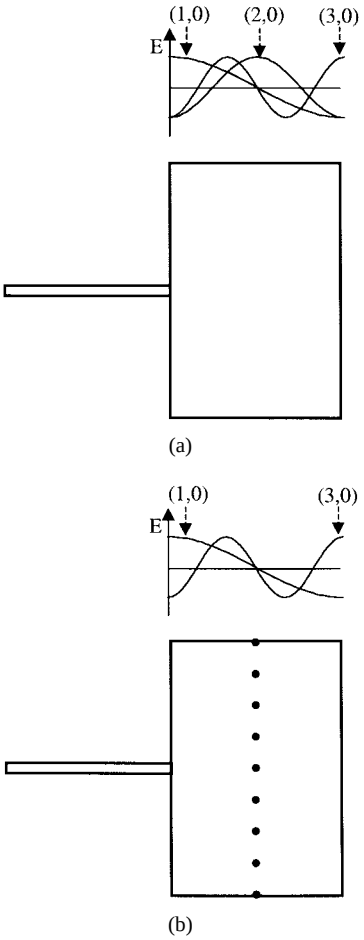

Fig. 3. Layout and mode distribution of (a) rectangular patch and (b) modified patch antenna.

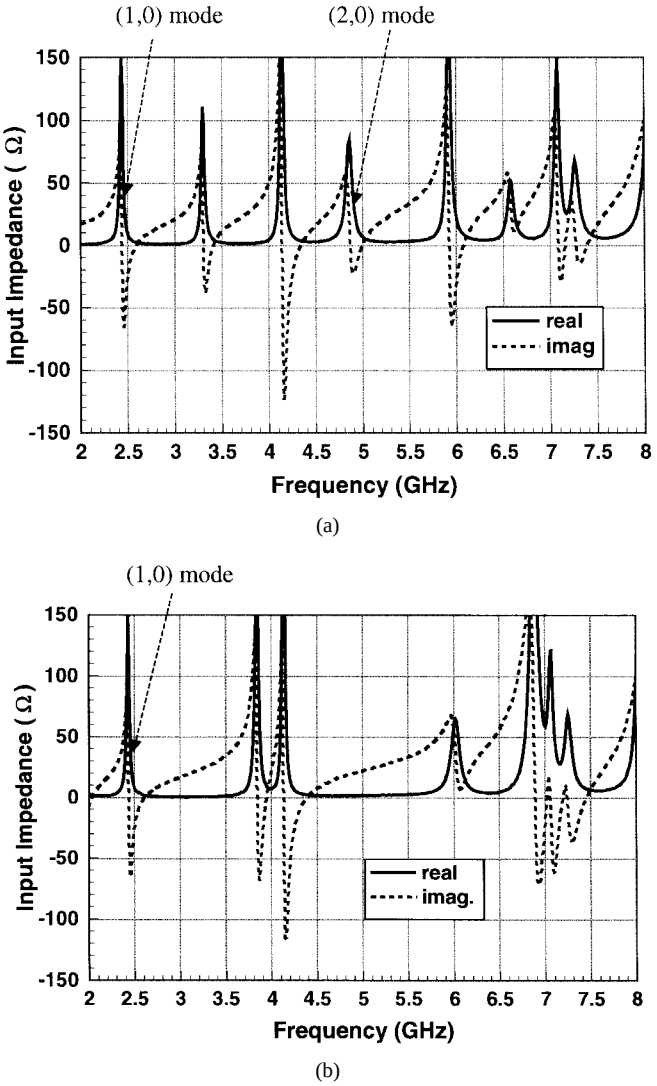

Fig. 4. (a) Measured input impedance of patch antenna. (b) Patch antenna with shorting pins. In both cases, the antenna is 1550-mil long and 2320-mil wide.

gain and radiation pattern for the chosen application. Also, low cross-polarization level at the fundamental frequency is essential. To prevent EMI, radiation at harmonic frequencies should be minimized.

To illustrate these antenna design guidelines, we will present two examples of antennas that are well suited for the active integrated-antenna approach. The first example consists of a rectangular patch antenna modified to eliminate a higher mode. The second example presents a circular-segment antenna. The linear relationship between modes is not maintained for patches of circular geometry.

Fig. 3(a) shows the geometry of a rectangular patch antenna and the mode profile for the (1, 0) and (2, 0) modes. The operating frequency is chosen slightly away from the resonance of the (1, 0) mode to avoid overly large input impedance. The second harmonic would, therefore, fall near the resonance of the (2, 0) mode. As stated previously, this is undesirable if the antenna is to be used for harmonic termination.

Fig. 3(b) shows the geometry of a rectangular patch antenna modified to eliminate the (2, 0) mode. Referring to the mode profiles in Fig. 3(a), the (2, 0)-mode electric field *peaks* at the center of the patch and the electric field of the (1, 0) mode is at *null*. Therefore, the (2, 0) mode can be eliminated by properly modifying the boundary conditions along the center line of the patch *without* affecting the (1, 0) mode. This is done by inserting a row of shorting pins along the center line [7]. From Fig. 4, which shows input impedance for both patch configurations, we can see that the resonance of the (2, 0) mode has been eliminated and that the real part of the input impedance is almost zero where the (2, 0) resonance should occur.

After modifying the input impedance of the antenna for optimal power-amplifier performance, we must ensure that the radiation properties have not degraded. Fortunately, the (1, 0) mode of the antenna is almost unchanged. Therefore, the radiation pattern of the patch with pins should be virtually the same as that of the regular patch. This is verified by measuring the normalized copolarization radiation pattern for both H- and E-planes, as shown in Fig. 5. The cross-polarization was also measured and was below -17 dB in all directions. The measured gain was 7.8 dB. These results are consistent with a conventional patch of the same dimensions operating near the (1, 0) resonance.

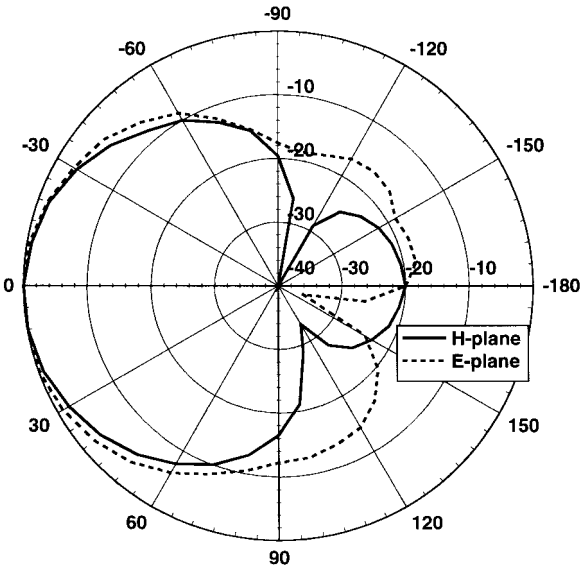

Fig. 5. Normalized H- and E-plane copolarization radiation pattern of patch antenna with shorting pins shown in Fig. 3(b).

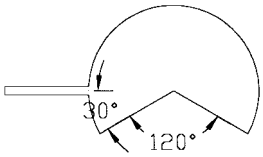

Fig. 6. Layout of the circular-sector microstrip antenna.

However, one disadvantage of the modified patch is that the (3, 0) mode remains unaffected by the shorting pins and is, therefore, not an ideal termination at the third harmonic of the power amplifier. If tuning of both harmonics is required in the amplifier design, another type of planar antenna must be utilized. A good choice is to use a planar antenna with circular geometry, such as annular, annular sector, or circular sector antennas [15]. Unlike rectangular geometry, the resonant frequencies for these antennas depend on the roots of Bessel functions, and antenna layouts can be optimized to offer tuning of both second and third harmonic.

One such example is a circular-sector microstrip antenna with 120° cut-out [16], as shown in Fig. 6. In the design of this antenna, both the sector angle as well as the angular location of the feed line are varied to provide appropriate input impedance. The measured input impedance of the circular-sector antenna is given in Fig. 7 for an antenna radius of 740 mil. As seen in Fig. 7, if the operating frequency f_0 is chosen near the first resonance, the real part of the input impedance will be small at both second and third harmonic. This antenna can, therefore, provide optimum input impedance at both the second and third harmonics, which is an advantage over rectangular geometry patch antennas.

Again, the radiation properties must be considered. The measured normalized copolarization radiation pattern is shown in Fig. 8. These patterns are acceptable for many wireless applications. Additionally, the cross-polarization for both H- and E-planes are found to be below -16 dB in all directions. The gain was measured to be 5.8 dB.

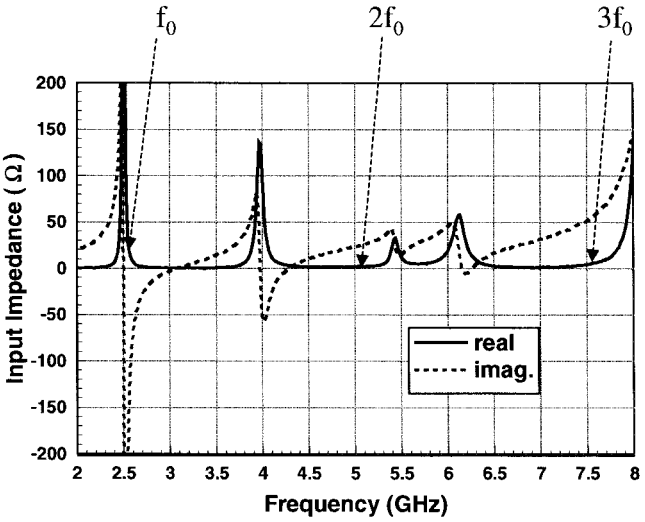

Fig. 7. Measured input impedance of the circular-sector microstrip antenna with radius of 740 mil. The system operating frequency is labeled f_0.

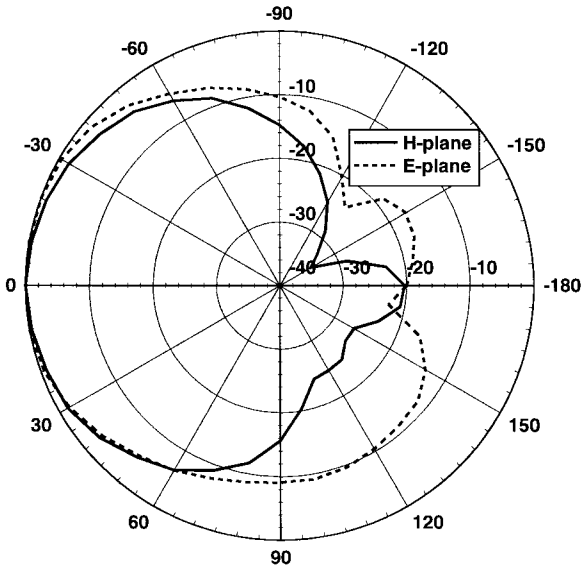

Fig. 8. Normalized H- and E-planes copolarization radiation pattern of circular sector antenna shown in Fig. 6.

B. Periodic-Structure Approach

Broad-band harmonic tuning is typically difficult to achieve for active integrated-antenna amplifiers and for power amplifiers in general. The technique of the previous section is typically narrow-band. Therefore, additional harmonic filtering is required for broad-band operation. For this purpose, structures with large transmission stopbands are required. Double-stub tuners or filters are conventionally used for harmonic tuning. Although any type of microstrip filter with appropriate broad-band characteristics can be used for harmonic tuning, we focus on a new type of microstrip filter based on removing portions of the microstrip ground plane. In addition to its broad-band performance and low losses, the top conductor can potentially be used for other purposes, such as matching. In this respect, these periodic structures promise to be a compact multifunctional microstrip structure.

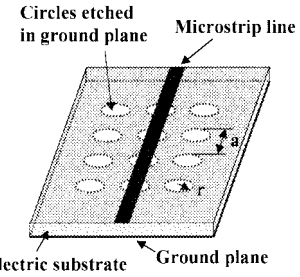

Fig. 9. 3-D view of the periodic structure used to tune harmonic for the periodic-structure approach. The ground plane has a square lattice with 4 × 3 etched circles. The circle radius is 110 mil and the period is 480 mil.

Design rules for microstrip-based PBG structures are similar to those of conventional PBG materials. One issue is to accurately predict the frequency response of these complex structures. Several design guidelines exist for doing this. First, the stopband center frequency $f_{\rm stop}$ is a function of the period of the structure. The guided wavelength at $f_{\rm stop}$ is twice the period a. Therefore, ($f_{\rm stop}$) is determined from the following equation:

$$f_{\rm stop} = \frac{c}{2a\dfrac{\beta}{\beta_0}} \tag{1}$$

where c is the speed of light, β is the propagation constant in the periodic structure, β_0 is the free-space propagation constant, and a is the period. A useful first-order approximation is that the propagation constant is simply that of the unperturbed microstrip transmission line. As will be shown later, this simple rule-of-thumb provides reasonable results. The second guideline roughly determines the depth and width of the stopband. Logically, using a larger number of periods increases the perturbation.

One recently developed periodic structure is shown in Fig. 9. The circles in the figure represent an etched 2-D pattern in the microstrip ground plane [12]. For simplicity, a square lattice is chosen. Perturbation shape is circular. As stated previously, the number of periods determines the depth of the stopband. Additionally, it has been experimentally shown that the radius (or length) r of the etched pattern also has some effect on stopband depth. Values of r within $0.15 < r/a < 0.25$ range are optimal. Smaller r causes smaller perturbation and smaller stopband dip. However, an overly large r/a ratio may actually be detrimental. For $r/a > 0.25$, the perturbation is too strong and causes significant ripples in the passband transmission. Intuitively, these effects are expected. In the limiting case that the r/a ratio approaches zero, we obtain the frequency response of unperturbed microstrip line. Alternatively, as r/a approaches infinity, the microstrip ground plane disappears and the microstrip mode will no longer be guided. It has also been experimentally shown that little or no radiation occurs from the holes etched in the ground plane. This is essential if the structure is to be used in wireless systems.

To demonstrate the value of these guidelines, a periodic structure design example is presented. The stopband center frequency is chosen at 8.8 GHz on a microstrip substrate

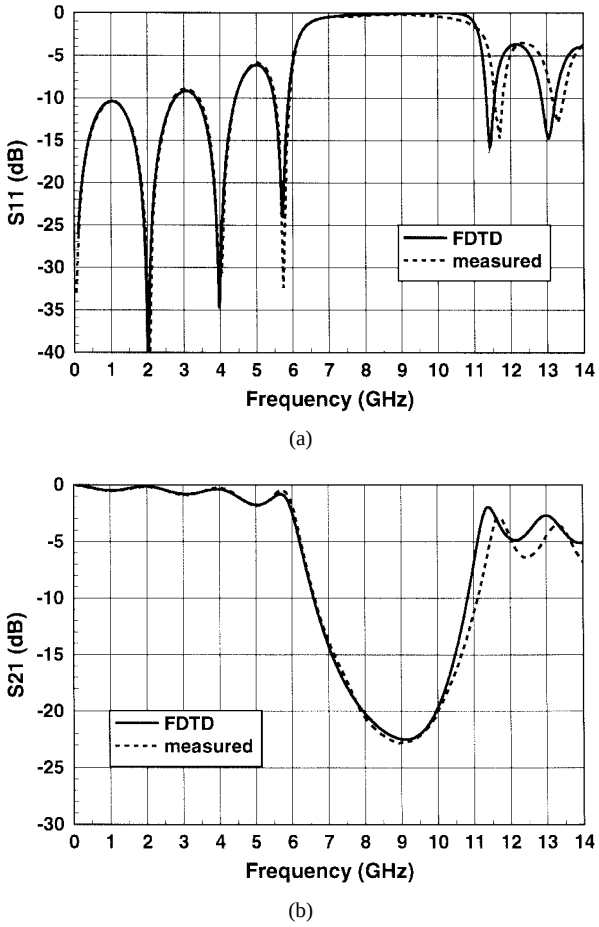

Fig. 10. FDTD simulated and measured (a) S_{11} and (b) S_{21} for the periodic structure shown in Fig. 9.

of permittivity 2.33 and a 31-mil substrate thickness. The lattice period is first determined from (1) for 50 Ω to be 480 mil. For optimal frequency response, an r/a ratio of 0.23 is chosen. This corresponds to a circle radius of 110 mil. No simple formula exists for determining the number of periods. This must be found either empirically or by using full-wave analysis. In our case, four periods are used which gives an S_{21} of at least −16 dB in the stopband.

Fig. 10 shows S-parameters for the periodic structure obtained by a full-wave FDTD simulation, as well as measured S-parameters obtained from an HP8510 network analyzer. In the FDTD simulation, metal and dielectric losses have been neglected. Additionally, the circles in the microstrip ground plane were modeled using staircase approximation. The maximum stopband depth is −22.5 dB at 9.08 GHz for FDTD and −22.8 dB at 8.93 GHz. Less than 2% error is obtained between measured and FDTD data for maximum stopband depth and good agreement is observed over the entire frequency span. Therefore, FDTD is an excellent tool to accurately model these structures. Another important concern is the accuracy of (1). If the propagation constant of unperturbed microstrip is used in (1), the stopband frequency is calculated to be 8.78 GHz, in close agreement with measurement. Therefore, in initial design stage, (1) can be used to calculate the lattice period. Then, broad-band frequency response should be obtained using a full-wave analysis, such as FDTD.

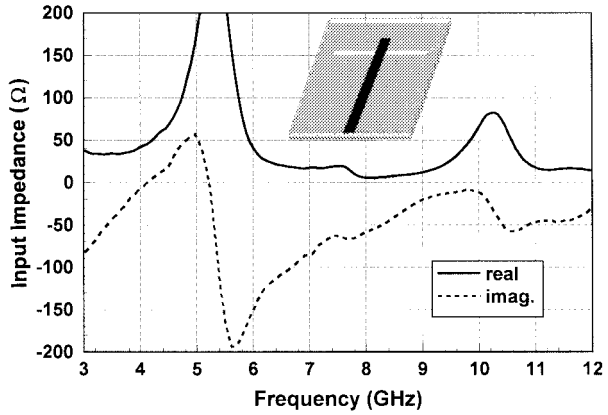

Fig. 11. Measured input impedance of the slot antenna with microstrip feed.

TABLE I
MEASURED SLOT ANTENNA GAIN

Freq. (GHz)	3.7	3.8	3.9	4.0
Gain (dB)	2.2	3.0	3.3	2.9

PBG-based periodic filters are typically broad-band, and can be used for broad-band harmonic tuning in either a 50-Ω environment or with an integrated antenna. One important factor is the bandwidth of the antenna, which may have a limiting effect on the system. Therefore, for maximum broad-band tuning in an integrated-antenna system, this should be combined with a broad-band antenna.

One such antenna is one wavelength (1λ) slot antenna. The 1λ slot is chosen because it has wider bandwidth than a $\lambda/2$ slot. This antenna has good radiation pattern and cross-polarization. The slot antenna is designed with a microstrip feed for operation in the 3.7–4.0-GHz range. The slot is 2200-mil long and 130-mil wide. Table I shows measured slot antenna gain for the frequency range of interest.

Input impedance is a crucial factor in the active integrated-antenna approach. Fig. 11 shows measured input impedance of the fabricated slot antenna. In the operating bandwidth, the real part of the input impedance is in the range of 32–42 Ω. At twice the operating frequency, maximum of the real part of the input impedance is approximately 20 Ω. Similarly, at three times the operating frequency, the maximum of the real part of the input impedance is approximately 45 Ω. Therefore, this antenna is not suited for termination of the second or third harmonics of a power amplifier. However, the bandwidth at the chosen operating point is considerably wider than that of any of the previously mentioned antennas. This antenna is, therefore, suitable for integration with periodic structure for broad-band harmonic tuning.

C. Combined Approach

One disadvantage of the periodic-structure method is that it can be used to tune only even or odd harmonics. Similarly, in the active integrated-antenna approach, it may be difficult to find antenna structures that have proper termination at both second and third harmonic. Combining the two approaches can eliminate these disadvantages. However, the antennas that have been examined for harmonic tuning are narrow-band, and this will limit the harmonic-tuning bandwidth of the system.

One possible example of this is the patch antenna with pins integrated with a periodic structure. The antenna is designed to tune the second harmonic of a power amplifier, while the periodic structure is used to tune the third harmonic. Choosing the periodic to tune the third harmonic allows a more compact structure between the amplifier and antenna to minimize losses.

The antenna chosen for the second harmonic tuning is the patch antenna with shorting pins (discussed in Section II-A). The operating frequency is chosen at 2.45 GHz, which is near the (1, 0) resonance. The periodic structure, similar to the one shown in Section II-B, is added at the feed to terminate the third harmonic. Since the third harmonic is at 7.35 GHz, the filter period is calculated from (1) to be 500 mil. The circle radius is 110 mil, which gives $r/a = 0.22$. Again, a 4×3 square lattice is used and gives S_{21} of -17.5 dB at the third harmonic. The real part of the input impedance of the cascaded periodic structure and patch is 1.4 Ω at the third harmonic, which is sufficiently low for third harmonic tuning.

III. POWER-AMPLIFIER EXAMPLES

To demonstrate the techniques of Section II, three amplifiers are designed and tested. Two class-AB power amplifiers are presented. One is a broad-band power amplifier integrated with a slot antenna, in which tuning of the second harmonic is achieved using the periodic filter. The second is a power amplifier integrated with a modified patch and periodic structure, in which tuning of both harmonics is achieved using a combined approach. Additionally, a class-F amplifier with AB biasing is presented. Proper design of class-F power amplifiers requires second and third harmonic tuning. Therefore, this can be used with the active antenna method (with the antenna tuning both harmonics) or with the combined method. This is demonstrated with a circular-sector antenna.

In all three cases, the amplifier was designed using Hewlett-Packard's microwave design system (MDS) harmonic-balance simulator. The periodic structure and/or antenna were incorporated into simulation as two- or one-port devices containing measured S-parameter data. The active device is microwave technology MWT-8HP power GaAs FET with gatewidth of 1.2 mm and is modeled using the built-in large-signal model available within MDS. The drain voltage is fixed to 5 V, since this value gives maximum PAE. The gate is biased so that the quiescent drain current is 10% I_{DSS}, which also gives maximum PAE for this device.

Measurements with an active antenna system are typically more difficult than with a conventional 50-Ω amplifier. The antenna and amplifier are combined into one circuit. Therefore, measurements must be done in an anechoic chamber with a receiving antenna. The amplifier output power and efficiency are calibrated using the Friis free-space transmission formula [19]. To do this, the gain of the passive antenna is first measured at broadside. This serves as a power calibration. The passive antenna is then substituted with the power amplifier integrated with an antenna. This measurement method eliminates any systematic errors. All amplifier results shown in the following

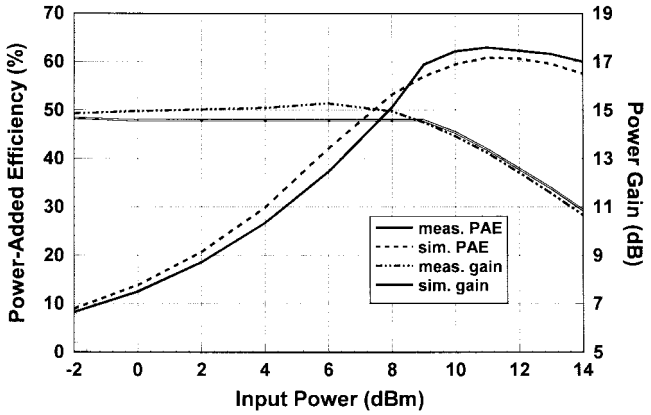

Fig. 12. Measured and simulated PAE and power gain versus input power for the power amplifier integrated with circular-segment antenna.

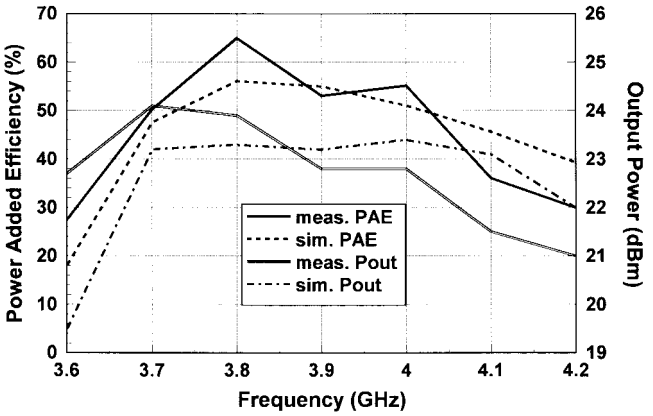

Fig. 13. Measured and simulated PAE and output power versus frequency for the broad-band power amplifier integrated with slot and periodic structure.

subsections are based on amplifier gain only, and do not include antenna gain.

A. Power Amplifier Using Active Integrated-Antenna Approach

In theory, the class-F amplifier acts as a perfect switch and generates a square-wave at the drain. Several practical concerns exist when designing a class-F amplifier. In practice, only second and third harmonics are considered when designing a class-F amplifier. This is because higher harmonics usually contain smaller amounts of power and do not contribute significantly to waveform shaping. At microwave frequencies, packaging parasitics become significant and must be compensated for in the output circuit. Therefore, the optimum second and third harmonic load are not pure short and open, respectively, but may have a significant reactance depending on device and amplifier configuration. Similarly, drain voltage waveform for the class-F amplifier will deviate from the ideal square voltage waveform. The overlap between current and voltage waveforms should be minimized in order to maximize efficiency.

The circular sector antenna, shown in Fig. 6, is chosen as a load for a class-F amplifier because it can provide both second and third harmonic termination. A simple matching circuit between the device drain and antenna brings the antenna impedance to an optimal value at the fundamental and two harmonic frequencies. Fig. 12 shows PAE and power gain versus input power at the operating frequency of 2.55 GHz [16]. Maximum measured PAE was 63% at output power of 24.4 dBm. From Fig. 12, we can see that this hybrid-simulation method shows excellent agreement with measurement at both small-signal (small input power) and large-signal (input power near saturation) operation.

B. Broad-Band Power Amplifier Using Periodic-Structure Method

For some applications, a broad-band power amplifier is required. One way is to use a single-ended amplifier with a broad-band harmonic tuner. The choice for the broad-band harmonic tuner is critical. We use the previously discussed periodic structure (shown in Fig. 9) because of its broad bandwidth. As mentioned previously, the bandwidth of the antenna has an overall limiting effect on system bandwidth. For this reason, the periodic structure is integrated with the slot antenna, shown in Fig. 11. A class-AB active antenna amplifier is designed using techniques similar to those in the previous example [17]. The periodic structure is used to tune the second harmonic. Fig. 13 shows PAE and output power versus frequency for the amplifier. The measured PAE is better than 50% over an 8% bandwidth (3.7–4.0 GHz) with second harmonic tuning only.

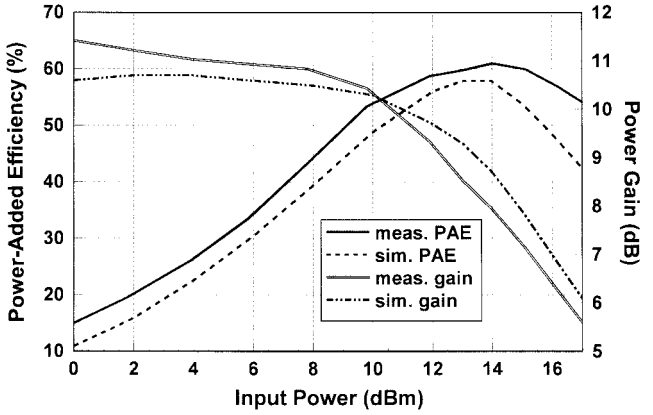

Fig. 14. Measured and simulated PAE and power gain versus input power for the combined approach power amplifier.

C. Power Amplifier Using Combined Approach

Higher efficiency is achieved by tuning both the second and third harmonics. This can be done using the combined method introduced in Section II-C. The microstrip patch with shorting pins is used to tune the second harmonic, and the periodic structure described in Section II-C is used to tune the third for a class-AB power amplifier [18]. Fig. 14 shows PAE and power gain versus input power at the operating frequency of 2.45 GHz. Maximum measured PAE was 61% at output power of 21.9 dBm. For reference purposes, a class-B power amplifier with a similar device and the same patch antenna with shorting pins (for second harmonic tuning only) showed

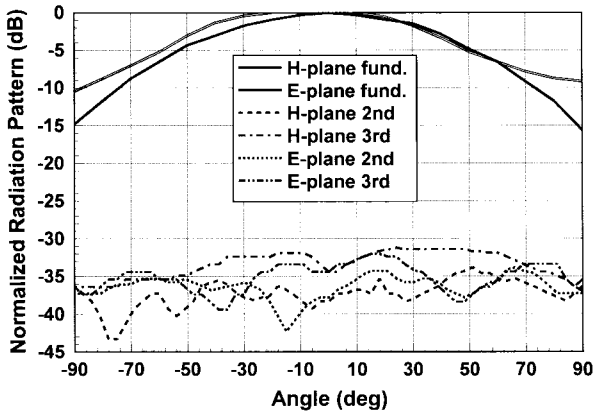

Fig. 15. Normalized H- and E-planes copolarization radiation pattern of fundamental, second and third harmonics for the class-F amplifier integrated with circular-sector antenna.

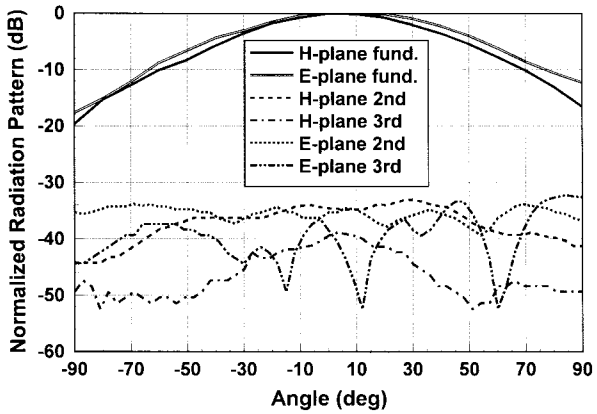

Fig. 16. Normalized H- and E-plane copolarization radiation pattern of fundamental, second, and third harmonics for the class-AB amplifier integrated with patch antenna with shorting pins.

measured PAE of 55%. Although not a systematic comparison, the difference in PAE is substantial [7].

IV. Harmonic-Radiation Reduction

Harmonic radiation is another important issue in wireless systems. Harmonic radiation is caused when the power amplifier generates significant harmonics, which may radiate through the antenna and, consequently, degrade system performance. One example where this effect can be a substantial problem is cosite interference, which may occur when a number of antennas operating at different frequencies are mounted in close proximity. Employing additional filters to solve the resulting EMI problem is not only expensive, but decreases the transmitter efficiency and may degrade the receiver noise figure.

The harmonic-tuning techniques presented here cannot only improve the amplifier efficiency, but also reduce unwanted harmonic radiation. This is observed by measuring the second and third harmonic radiation from the amplifiers presented in Sections III-A and III-C. Since harmonic frequencies may have a different radiation pattern from that of the fundamental, the harmonic-radiated power has to be measured in all directions, as shown in Figs. 15 and 16. For the power amplifier integrated with a circular-sector antenna, the second and third harmonics were 33.8 and 31.4 dB below the fundamental-frequency peak power, as shown in Fig. 15. For the power amplifier integrated with patch (with pins) and PBG, the second harmonic was 33.1 dB and the third was 32.2 dB below the fundamental-frequency peak power, as shown in Fig. 16. In both cases, the input power is set for maximum PAE. The output power is calibrated using receiving antenna gain and the Friis transmission formula at corresponding frequencies. Therefore, the fundamental and harmonic power levels are referenced at the output of the antenna integrated with amplifier.

V. Conclusion

In this paper, three new architectures for high-efficiency wireless amplifiers have been demonstrated. These techniques rely on either using the characteristics of the transmitting antenna to replace conventional harmonic tuning and matching circuitry or to use a new type of filter. These techniques minimize system complexity and allow compact and highly efficient designs. Additionally, these techniques have been shown to reduce EMI by preventing harmonic radiation.

The first method is based on active integrated-antenna approach, and uses the antenna's input impedance to tune harmonics. This technique results in minimal circuitry, but is limited by the bandwidth of the antenna and is typically narrow-band. This method can be used to design class-AB, class-B, class-C, or class-F power amplifiers. In this paper, a class-F operation is presented with harmonic tuning of both the second and third harmonic through the antenna input impedance.

The second approach incorporates a novel microstrip periodic structure based on etching a periodic pattern in the microstrip ground plane. This structure has a wide stopband in the transmission coefficient, which can be used for either second or third harmonic tuning. FDTD simulation results and simple guidelines for designing this structure are also given. As an example, a broad-band class-AB power amplifier integrated with a slot antenna is presented. The disadvantage of this approach is that it adds an additional filter between amplifier device and antenna. However, this technique has been shown to be more broad-band than the active integrated-antenna approach and conventional stub-filter method. Additionally, because the periodic structure is located purely on the ground plane of the microstrip, the top conductor can potentially be used for matching between the antenna and device. This would result in a dual-purpose structure for minimal circuit size.

The third approach is the combination of the two above: one harmonic is tuned through the input impedance of the antenna and another using a periodic structure. This method can be used to design tuned class-AB, class-B, or class-C amplifiers, as well as class-F amplifiers. A tuned class-AB power amplifier integrated with a modified patch antenna and periodic structure is given as an example. Again, the overall system bandwidth is typically limited by the bandwidth of the antenna structure. However, higher efficiency levels are attainable when both harmonics are tuned.

These techniques make possible more compact and highly efficient designs through increased circuit integration. However, these benefits come at the expense of a more complicated design process. The integrated-antenna power-amplifier designer must have expertise in both power-amplifier design as well as antenna design. Additionally, more complex design techniques must be utilized. Design of these systems requires that the data obtained from full-wave analysis and experimental verification of the antenna structures be incorporated into the power-amplifier design process. However, new and exciting circuit topologies are possible with greatly reduced circuit space and increased efficiency.

REFERENCES

[1] J. Lin and T. Itoh, "Active integrated antennas," *IEEE Trans. Microwave Theory Tech.*, vol. 42, pp. 2186–2194, Dec. 1994.

[2] B. Kopp and D. D. Heston, "High efficiency 5-W power amplifier with harmonic tuning," in *IEEE MTT-S Int. Microwave Dig.*, New York, NY, May 1988, pp. 839–842.

[3] G. Hanington, P. F. Chen, V. Radisic, T. Itoh, and P. M. Asbeck, "A 10-MHz HBT DC–DC converter for microwave power amplifier efficiency improvement," in *IEEE MTT-S Int. Microwave Dig.*, Baltimore, MD, June 1998, vol. 2, pp. 589–592.

[4] J. R. Lane, R. G. Freitag, H.-K. Hahn, J. E. Degenford, and M. Cohn, "High-efficiency 1-, 2-, and 4-W class-B FET power amplifiers," *IEEE Trans. Microwave Theory Tech.*, vol. MTT-34, pp. 1318–1325, Dec. 1986.

[5] C. Duvanaud, S. Dietsche, G. Pataut, and J. Obregon, "High-efficiency class-F GaAs FET amplifier operating with very low bias voltage for use in mobile telephones at 1.75 GHz," *IEEE Microwave Guided Wave Lett.*, vol. 3, pp. 268–270, Aug. 1993.

[6] E. Camargo and R. M. Steinberg, "A compact high power amplifier for handy phones," *IEEE MTT-S Int. Microwave Symp. Dig.*, vol. 2, San Diego, CA, May 1994, pp. 565–568.

[7] V. Radisic, S. T. Chew, Y. Qian, and T. Itoh, "High efficiency power amplifier integrated with antenna," *IEEE Microwave Guided Wave Lett.*, vol. 7, pp. 39–41, Feb. 1997.

[8] J. D. Joannopoulos, R. D. Meade, and J. N. Winn, *Photonic Crystals: Molding the Flow of Light.* Princeton, NJ: Princeton Univ. Press, 1995.

[9] E. Yablanovich, "Inhibited spontaneous emission in solid-state physics and electronics," *Phys. Review Lett.*, vol. 58, no. 20, pp. 2059–2062, May 1987.

[10] L. J. Jasper and G. T. Tran, "Photonic band gap (PBG) technology for antennas," *Proc. SPIE—Int. Soc. Opt. Eng.*, vol. 2843, no. 4, pp. 80–89, Aug. 1996.

[11] D. R. Smith, S. Schultz, N. Kroll, M. Sigalas, K. M. Ho, and C. M. Soukoulis, "Experimental and theoretical results for a two-dimensional metal photonic band-gap cavity," *Appl. Phys. Lett.*, vol. 65, no. 5, pp. 645–647, Aug. 1994.

[12] V. Radisic, Y. Qian, R. Coccioli, and T. Itoh, "Novel 2-D photonic bandgap structure for microstrip lines," *IEEE Microwave Guided Wave Lett.*, vol. 8, pp. 69–71, Feb. 1998.

[13] T. B. Mader, M. Markovic, and Z. B. Popovic, "The transmission-line high-efficiency class-E amplifier," *IEEE Microwave Guided Wave Lett.*, vol. 5, pp. 290–292, Sept. 1995.

[14] Z. B. Popovic, "High efficiency microwave amplifiers and oscillators," in *MURI Low Power, Low Noise Electron. Mobile Wireless Commun.*, Annu. Rev., Univ. California Los Angeles, Oct. 1997.

[15] W. F. Richards, J. D. On, and S. A. Long, "A theoretical and experimental investigation of annular, annular sector, and circular sector microstrip antennas," *IEEE Trans. Antennas Propagat.*, vol. AP-32, pp. 864–867, Aug. 1984.

[16] V. Radisic, Y. Qian, and T. Itoh, "Class F power amplifier integrated with circular sector microstrip antenna," in *IEEE MTT-S Int. Microwave Dig.*, vol. 2, Denver, CO, June 1997, pp. 687–690.

[17] ——, "Broad-band power amplifier integrated with slot antenna and novel harmonic tuning structure," in *IEEE MTT-S Int. Microwave Symp. Dig.*, vol. 3, Baltimore, MD, June 1998, pp. 1895–1898.

[18] V. Radisic and T. Itoh, "Active antenna power amplifier with PBG," in *28th European Microwave Conf. Dig.*, vol. 1, Amsterdam, The Netherlands, Oct. 1998, pp. 156–160.

[19] C. A. Balanis, *Antenna Theory: Analysis and Design.* New York: Harper & Row, 1982.

Vesna Radisic received the B.S.E.E. degree from the University of Belgrade, Belgrade, Yugoslavia, in 1991, the M.S.E.E. degree from the University of Colorado at Boulder, in 1993, and is currently working toward the Ph.D. degree in electrical engineering at the University of California at Los Angeles (UCLA).

From 1994 to 1995, she was with the Ortel Corporation, where she was involved with broadband RF/fiber-optic transmitters and receivers. Her current research interests include microwave circuit and active antenna design.

Ms. Radisic received third place in the Student Paper Competition at the 1998 IEEE International Microwave Symposium.

Yongxi Qian (S'91–M'93), for photograph and biography, see this issue, p. 1900.

Tatsuo Itoh (S'69–M'69–SM'74–F'82–LF'94), for photograph and biography, see this issue, p. 1900.